Production of the pentaquark Θ^+ in np scattering

Seung-Il Nam,[1,2,∗] Atsushi Hosaka,[1,†] and Hyun-Chul Kim[2,‡]

^{1}Research Center for Nuclear Physics (RCNP), Ibaraki, Osaka 567-0047, Japan
^{2}Department of Physics and Nuclear physics & Radiation technology Institute (NuRI),
Pusan National University, Busan 609-735, Korea
(Dated: February 1, 2008)

Abstract

We study $np \to \Lambda\Theta^+$ and $np \to \Sigma^0\Theta^+$ processes for both of the positive and negative parities of the Θ^+. Employing the effective chiral Lagrangians for the KNY and K^*NY interactions, we calculate differential cross sections as well as total cross sections for the $np \to \Sigma^0\Theta^+$ and $np \to \Lambda\Theta^+$ reactions. The total cross sections for the positive-parity Θ^+ turn out to be approximately ten times larger than those for the negative parity Θ^+ in the range of the CM energy $\sqrt{s}_{\rm th} \le \sqrt{s} \le 3.5\,{\rm GeV}$. The results are rather sensitive to the mechanism of K exchanges in the t – channel.

∗Electronic address: sinam@rcnp.osaka-u.ac.jp
†Electronic address: hosaka@rcnp.osaka-u.ac.jp
‡Electronic address: hchkim@pusan.ac.kr

I. INTRODUCTION

Since the experimental finding of the lightest *pentaquark* baryon Θ^+ [1] motivated by the work of Ref. [2], the physics of the pentaquark states has been a hot issue. The DIANA [3], CLAS [4], SAPHIR [5], HERMES [6], SVD [7] collaborations and the reanalysis of neutrino data [8] have confirmed its existence. The Θ^+ has unique features: It has a relatively small mass and a very narrow width. The exotic Ξ states found recently by the NA49 collaboration [9] share the features similar to the Θ^+. While a great amount of theoretical effort has been put into understanding properties of the Θ^+ [10, 11, 12, 13, 14, 15, 16], there is no consensus in determining the parity of the Θ^+. For example, chiral models predict the parity of the Θ^+ to be positive [11], whereas the lattice QCD and the QCD sum rule prefer the negative parity [14, 15].

Many works have suggested different ways of determining the parity of the Θ^+ [18, 19, 20, 21, 22, 23, 24, 25, 26], among which Thomas *et al.* [19] have proposed an unambiguous method to determine the parity of the Θ^+ via polarized proton-proton scattering at and just above threshold of the Θ^+ and Σ^+: If the parity of the Θ^+ is positive, the reaction is allowed at the threshold region only when the total spin of the two protons is $S = 0$, while negative the reaction is allowed only when $S = 1$. Hence it is very challenging to measure such a process experimentally [27]. Triggered by Thomas *et al.* [19], Hanhart *et al.* [20] have extended the work of Ref. [19] to determine the parity of the Θ^+, asserting that the sign of the spin correlation function A_{xx} agrees with the parity of the Θ^+ near threshold. Similarly, Rekalo and Tomasi-Gustafsson [26] have put forward methods for the determination of the parity of the Θ^+ by measuring the spin correlation coefficients in three different reactions, *i.e.* $pn \to \Lambda\Theta^+$, $pp \to \Sigma^+\Theta^+$, and $pp \to \pi^+\Lambda\Theta^+$. Thus, it seems that the NN reactions provide a promising framework to determine the parity of the Θ^+. The present authors have performed the calculation of the cross sections of the reaction $\vec{p}\vec{p} \to \Sigma^+\Theta^+$ near the production threshold [24], finding that the cross sections for the allowed spin configuration are estimated to be of order of one microbarn for the positive parity Θ^+ and about one tenth microbarn for the negative parity Θ^+ in the vicinity of threshold, where the S-wave component dominates.

There exist already investigations on the production of the Θ^+ in the NN interaction [28, 29, 30, 31]. Refs. [29, 30] are concerned with the prediction of the total cross sections and Ref. [31] has explored the Θ^+ production in high-energy pp scattering. In the present work, we want to investigate the $np \to \Lambda\Theta^+$ and $np \to \Sigma^0\Theta^+$ processes with both of the positive and negative parities considered.

The present paper is organized as follows: In Section II, we shall compute the relevant invariant amplitudes from which the total and differential cross sections can be derived. In the subsequent section, we shall present the numerical results and discuss them. In the last section, we shall summarize and draw a conclusion.

II. EFFECTIVE LAGRANGIANS AND AMPLITUDES

The pertinent schematic diagrams for the $np \to Y^0\Theta^+$ reaction are drawn in Fig.1. At the tree level we can consider Born diagrams of pseudoscalar K and vector K^* exchanges. As mentioned before, we treat the reactions in the case of positive- and negative-parity Θ^+. We distinguish the positive-parity Θ^+ from the negative-parity one by expressing them as Θ^+_+ and Θ^+_-, respectively.
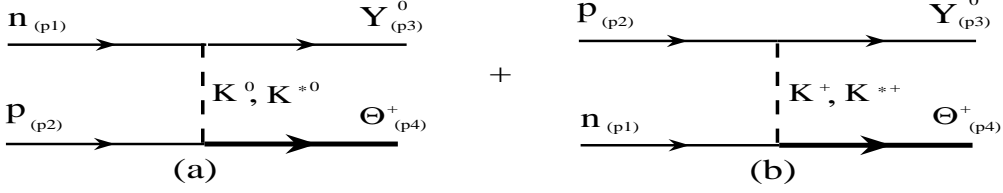
FIG. 1: Schematic diagrams for the $np \to Y^0\Theta^+$ reaction

We start with the following effective Lagrangians:

$$
\begin{aligned}
\mathcal{L}_{KNY} &= -ig_{KNY}\bar{Y}\gamma_5 K^\dagger N, \\
\mathcal{L}_{KN\Theta_\pm} &= -ig_{KN\Theta_\pm}\bar{\Theta}_\pm\Gamma_5 KN, \\
\mathcal{L}_{VNY} &= -g_{VNY}\bar{Y}\gamma_\mu V^\mu N - \frac{g^T_{VNY}}{M_Y + M_N}\bar{Y}\sigma_{\mu\nu}\partial^\nu V^\mu N, \\
\mathcal{L}_{VN\Theta} &= -g_{VN\Theta_\pm}\bar{\Theta}_\pm\gamma_\mu\bar{\Gamma}_5 V^\mu N - \frac{g^T_{VN\Theta_\pm}}{M_\Theta + M_N}\bar{\Theta}_\pm\sigma_{\mu\nu}\bar{\Gamma}_5\partial^\nu V^\mu N,
\end{aligned} \tag{1}
$$

where Y, K, N, Θ, and V stand for the hyperon (Σ^0 and Λ), kaon, nucleon, Θ^+, and vector meson fields, respectively. In order to take into account different parities for the Θ^+ in the reactions, we introduce $\Gamma_5 = \gamma_5$ for the Θ^+_+ and $\Gamma_5 = \mathbf{1}_{4\times 4}$ for the Θ^+_-. $\bar{\Gamma}_5$ designates $\Gamma_5\gamma_5$. The isospin factor is included in Y. The $KN\Theta$ coupling constant can be determined, if we know the deacy width $\Gamma_{\Theta\to KN}$. If we choose $\Gamma_{\Theta\to KN} = 15\,\mathrm{MeV}$ together with $M_\Theta = 1540\,\mathrm{MeV}$ [1], we find that $g_{KN\Theta^+_+} = 3.78$ and $g_{KN\Theta^+_-} = 0.53$. If one takes a different width for $\Gamma_{\Theta\to KN}$, the coupling constant scales as a square root of the width. As for the unknown coupling constant $g_{K^*N\Theta}$, we follow Ref. [32], i.e., $g_{K^*N\Theta} = \pm|g_{KN\Theta}|/2$. The tensor coupling constant $g^T_{K^*N\Theta}$ is then fixed as follows: $g^T_{K^*N\Theta} = \pm|g_{KN\Theta}|$ as in Ref. [24]. Since the sign of the coupling constants cannot be fixed by SU(3) symmetry, we shall use both signs [32]. We employ the values of the KNY and K^*NY coupling constants referring to those from the new Nijmegen potential [33] as well as from the Jülich–Bonn potential [34] as summarized in Table. I.

	$g_{KN\Lambda}$	$g_{K^*N\Lambda}$	$g^T_{K^*N\Lambda}$	$g_{KN\Sigma}$	$g_{K^*N\Sigma}$	$g^T_{K^*N\Sigma}$
Nijmegen	-13.26	-5.19	-13.12	3.54	-2.99	2.56
Jülich–Bonn	-18.34	-5.63	-18.34	5.38	-3.25	7.86

TABLE I: The coupling constants

The invariant Feynman amplitudes corresponding to Fig. 1 are obtained as follows:

$$
\begin{aligned}
i\mathcal{M} = \Bigg[& i\frac{F^2(q^2)g_{KYN}g_{KN\Theta_\pm}}{q^2 - M_K^2}\bar{u}(p_4)\Gamma_5 u(p_2)\bar{u}(p_3)\gamma_5 u(p_1) \\
+ & i\frac{F^2(q^2)g_{K^*YN}g_{K^*N\Theta_\pm}}{q^2 - M_{K^*}^2}\left(\bar{u}(p_4)\gamma^\mu\bar{\Gamma}_5 u(p_2)\bar{u}(p_3)\gamma_\mu u(p_1) - \frac{1}{M_{K^*}^2}\bar{u}(p_4)\slashed{q}\bar{\Gamma}_5 u(p_2)\bar{u}(p_3)\slashed{q}u(p_1)\right) \\
- & i\frac{F^2(q^2)g^T_{K^*YN}g_{K^*N\Theta_\pm}}{2(M_N + M_Y)(q^2 - M_{K^*}^2)}\bar{u}(p_4)\gamma^\mu\bar{\Gamma}_5 u(p_2)\bar{u}(p_3)(\gamma_\mu\slashed{q} - \slashed{q}\gamma_\mu)u(p_1)
\end{aligned}
$$

3

$$+ \; i\frac{F^2(q^2)g_{K^*YN}g_{K^*N\Theta_\pm}^T}{2(M_N + M_\Theta)\left(q^2 - M_{K^*}^2\right)}\bar{u}(p_4)\bar{\Gamma}_5(\gamma^\mu\slashed{q} - \slashed{q}\gamma^\mu)u(p_2)\bar{u}(p_3)\gamma_\mu u(p_1)$$

$$- \; i\frac{F^2(q^2)g_{K^*YN}^T g_{K^*N\Theta_\pm}^T}{4(q^2 - M_{K^*}^2)(M_N + M_Y)(M_N + M_\Theta)}\bar{u}(p_4)(\gamma^\mu\slashed{q} - \slashed{q}\gamma^\mu)\bar{\Gamma}_5 u(p_2)\bar{u}(p_3)(\gamma_\mu\slashed{q} - \slashed{q}\gamma_\mu\slashed{q})u(p_1)\Bigg]$$

$$+ \; \left[p_1 \leftrightarrow p_2\right], \tag{2}$$

where $q = p_1 - p_3$. In order to compute the cross sections for these reactions, we need the form factors at each vertex to take into account the extended size of hadrons. For the Nijmegen potential we introduce the monopole-type form factor [35] in the form of

$$F(q^2) = \frac{\Lambda^2 - m^2}{\Lambda^2 - t}, \tag{3}$$

where m and t are the meson mass and a squared four momentum transfer, respectively. The value of the cutoff parameter is taken to be 1.0 GeV for the parameter set of the Nijmegen potential [24]. As for that of the Jülich–Bonn potential, we make use of the following form factor taken from Ref. [34]:

$$F(q^2) = \frac{\Lambda^2 - m^2}{\Lambda^2 + |\mathbf{q}|^2}, \tag{4}$$

where $|\mathbf{q}|$ is the three momentum transfer. In this case, we take different values of the cutoff masses for each KNY vertex as follows [34]: $\Lambda_{KN\Theta} = \Lambda_{K^*N\Theta} = 1.0\,\mathrm{GeV}$, $\Lambda_{KN\Lambda} = 1.2\,\mathrm{GeV}$, $\Lambda_{K^*N\Lambda} = 2.2\,\mathrm{GeV}$, $\Lambda_{KN\Sigma} = 2.0\,\mathrm{GeV}$, and $\Lambda_{K^*N\Sigma} = 1.07\,\mathrm{GeV}$.

III. NUMERICAL RESULTS AND DISCUSSION

In this section, we present the total and differential cross sections for the reactions $np \rightarrow \Lambda^0\Theta^+$ and $np \rightarrow \Sigma^0\Theta^+$ with two different parities of Θ^+. We first consider the case of parameter set of the Nijmegen potential. In Fig. 2, we draw the total cross sections of
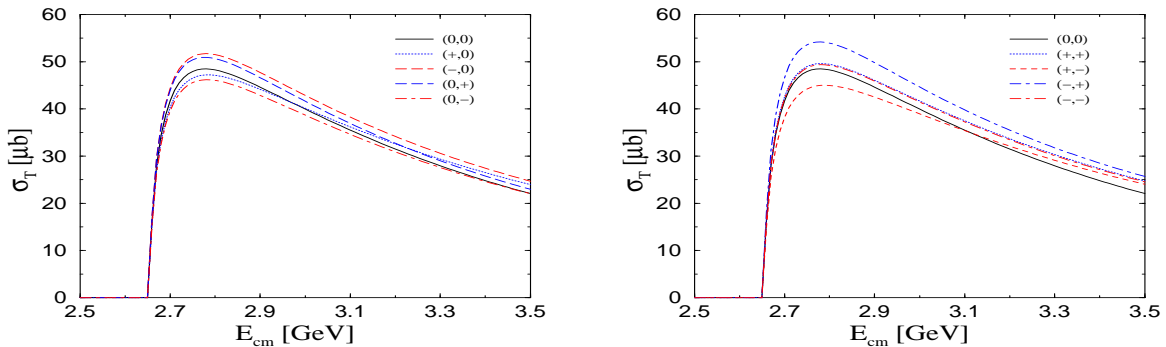

FIG. 2: The total cross sections of $np \rightarrow \Lambda\Theta_+^+$ with ten different combinations of the signs of the $K^*N\Theta$ coupling constants which are labeled by $(\mathrm{sgn}(g_{K^*N\Theta}), \mathrm{sgn}(g_{K^*N\Theta}^T))$. The parameter set of the Nijmegen potential with the cutoff parameter $\Lambda = 1.0$ GeV is employed.

$np \rightarrow \Lambda\Theta_+^+$ for different signs of the coupling constants, which are labeled as $(\mathrm{sgn}(g_{K^*N\Theta}),$

4

$\text{sgn}(g_{K^*N\Theta}^T)$). We compare the results from ten different combinations of the signs. As shown in Fig. 2, the dependence on the signs is rather weak. Moreover, we find that the contribution from K^* exchange is very tiny. The average total cross section is obtained as $\sigma_{np\to\Lambda\Theta_+^+} \sim 40~\mu b$ in the range of the CM energy $\sqrt{s}_{\text{th}} \leq \sqrt{s} \leq 3.5$ GeV, where $\sqrt{s}_{\text{th}} = 2656$ MeV. Since the angular distribution for all reactions is with a similar shape, we show the results only for the case of $np \to \Lambda\Theta_+^+$ in Fig. 3.

FIG. 3: The differential cross sections for the reaction $np \to \Lambda\Theta_+^+$ at $\sqrt{s} = 2.7$ GeV with five different combinations of the signs of the $K^*N\Theta$ coupling constants as labeled by $(\text{sgn}(g_{K^*N\Theta}),$ $\text{sgn}(g_{K^*N\Theta}^T))$. The parameter set of the Nijmegen potential with the cutoff parameter $\Lambda = 1.0$ GeV is employed.
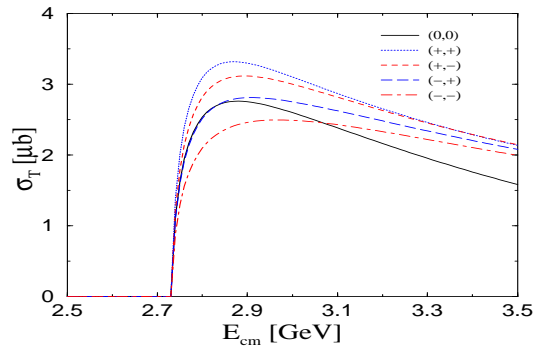

FIG. 4: The total cross sections for the reaction $np \to \Sigma^0\Theta_+^+$. The parameter set of the Nijmegen potential with the cutoff parameter $\Lambda = 1.0$ GeV is employed. The notations are the same as in Fig. 3.

In Fig. 4, we draw the total cross sections for the reaction $np \to \Sigma^0\Theta_+^+$. We find that they are about ten times smaller than those for the reaction $np \to \Lambda\Theta_+^+$. The corresponding average total cross section is found to be $\sigma_{np\to\Sigma^0\Theta_+^+} \sim 2.0~\mu b$ in the range of the CM energy $\sqrt{s}_{\text{th}} \leq \sqrt{s} \leq 3.5$ GeV, where $\sqrt{s}_{\text{th}} = 2733$ MeV. It can be easily understood from the fact that the ratio of the coupling constants $|g_{KN\Lambda}/g_{KN\Sigma}| = 3.74$ is rather large and the contribution from K-exchange is dominant.

As for the negative parity Θ^+, we show the results in Fig. 5. Once again we find that the contribution of K^* exchange plays only a minor role. We observe in average that $\sigma_{np\to\Lambda\Theta_-^+} \sim$

5

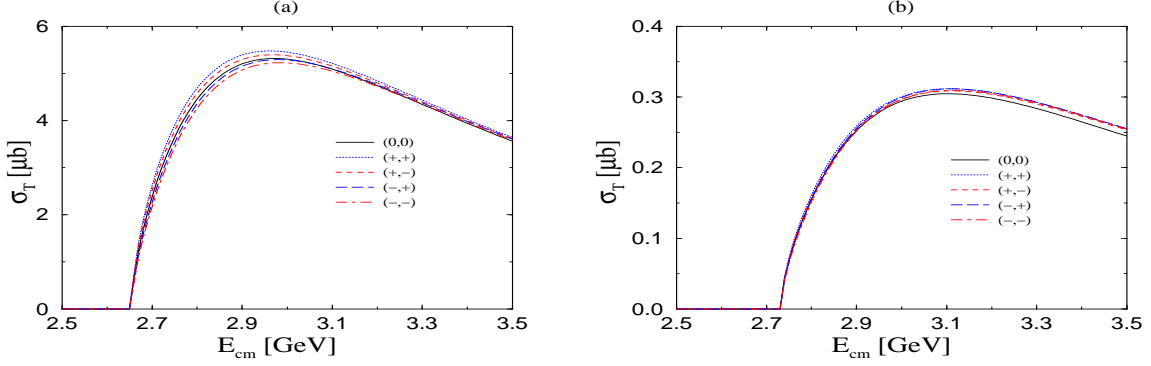FIG. 5: The total cross sections of $np \to \Lambda\Theta_-^+$ in the left panel (a) and $np \to \Sigma^0\Theta_-^+$ in the right panel (b). The parameter set of the Nijmegen potential with the cutoff parameter $\Lambda = 1.0$ GeV is employed. The notations are the same as in Fig. 3.

5.0 μb and $\sigma_{np\to\Sigma^0\Theta_-^+} \sim 0.3$ μb in the range of the CM energy $\sqrt{s}_{\text{th}} \leq \sqrt{s} \leq 3.5$ GeV. They are almost ten times smaller than those of Θ_+^+. This behavior can be interpreted dynamically by the fact that a large momentum transfer ~ 800 MeV enhances the P-wave coupling of the Θ_+^+ than the S-wave one of the Θ_+^+.

In Fig. 6, we show the total cross sections of the reactions for the $\Theta_\pm^+$ with the parameter set of the Jülich–Bonn potential. Here, different cutoff parameters are employed at different vertices as mentioned previously. We find that the contribution from K^* exchange turns
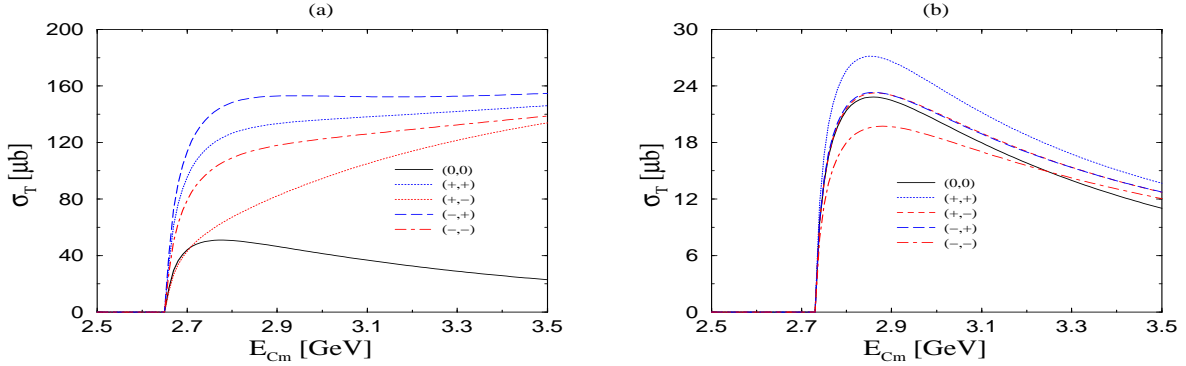

FIG. 6: The total cross sections of $np \to \Lambda\Theta_+^+$ in the left panel (a) and $np \to \Sigma^0\Theta_+^+$ in the right panel (b). The parameter set of the Jülich–Bonn potential is employed. The notations are the same as in Fig. 3.

out to be larger in the $np \to \Lambda\Theta_+^+$ reaction than in the $np \to \Sigma^0\Theta_+^+$. This can be easily understood from the fact that the Jülich–Bonn cutoff parameter $\Lambda_{K^*N\Lambda}$ is chosen to be approximately twice as large as that of the $KN\Lambda$ vertex, while the value of the $\Lambda_{K^*N\Sigma}$ is about two times smaller than that of the $\Lambda_{KN\Sigma}$. The average total cross sections are obtained as follows: $\sigma_{np\to\Lambda\Theta_+^+} \sim 100$ μb and $\sigma_{np\to\Sigma^0\Theta_+^+} \sim 20$ μb in the range of the CM energy $\sqrt{s}_{\text{th}} \leq \sqrt{s} \leq 3.5$ GeV.

In Fig. 7, the total cross sections for Θ_-^+ are drawn. In this case, the average total cross sections are given as follows: $\sigma_{np\to\Lambda\Theta_+^+} \sim 6.0$ μb and $\sigma_{np\to\Sigma^0\Theta_+^+} \sim 2.0$ μb in the same range of
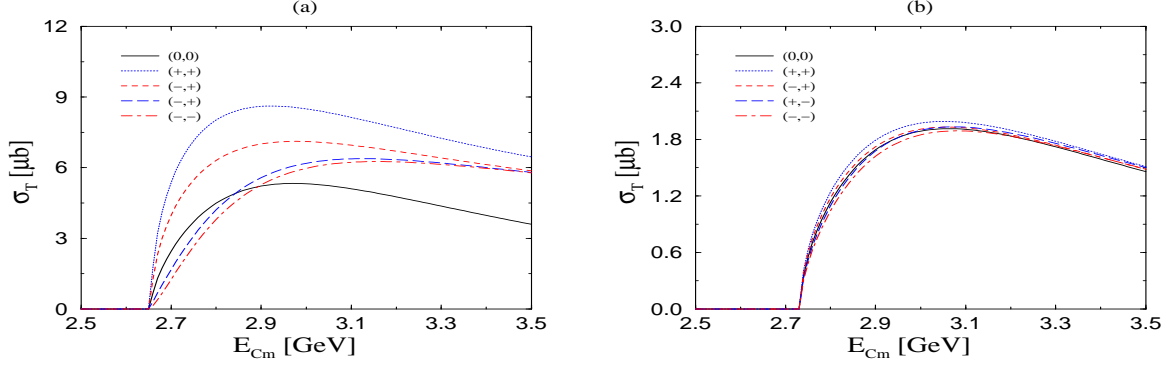
FIG. 7: The total cross sections of $np \to \Lambda\Theta^+_-$ in the left panel (a) and $np \to \Sigma^0\Theta^+_-$ in the right panel (b). The parameter set of the Jülich–Bonn potential is employed. The notations are the same as in Fig. 3.

the CM energy. The results for the negative-parity Θ^+_- are about fifteen times smaller than those of Θ^+_+.

Compared to the results with the parameter set of the Nijmegen potential, those with the Jülich–Bonn one are rather sensitive to the signs of the coupling constants. It is due to the fact that the cutoff parameters taken from the Jülich–Bonn potential are different at each vertex. If we had taken similar values of the cutoff parameters for the Nijmegen potential, we would have obtained comparable results to the case of the Jülich-Bonn potential.

IV. SUMMARY AND CONCLUSION

Motivated by a series of recent works [18, 19, 20, 21, 22, 23, 24, 25, 26], we have studied the reactions $np \to \Lambda\Theta^+$ and $np \to \Sigma^0\Theta^+$, employing both of the negative and positive parities for the Θ^+. We have considered K and K^* meson exchanges in the Born approximation. The coupling constant for the $KN\Theta$ vertex has been fixed by using experimental information on the width $\Gamma_{\Theta\to KN}$ as well as the mass M_Θ, while those for K^* exchange have been estimated by using SU(3) symmetry [32]. It turned out that the contribution of K exchange was dominant and that the overall results were rather insensitive to the value of the cutoff parameter Λ. In conclusion, we have found that $\sigma_{np\to Y^0\Theta^+_+} >> \sigma_{np\to Y^0\Theta^+_-}$, as shown in Table. II where we have summarized the average total cross sections.

	Nijmegen		Jülich-Bonn	
Final Hyperon	Λ	Σ^0	Λ	Σ^0
$\sigma_{P=+1}\,[\mu b]$	40	2.0	100	20
$\sigma_{P=-1}\,[\mu b]$	5.0	0.3	6.0	2.0

TABLE II: The average total cross sections

As suggested by Refs. [19, 20, 21, 22, 24, 25, 26], the NN interaction will provide a good framework to determine the parity of the Θ^+, though it might still require an experimental challenge. However, we anticipate that we would provide a guideline together with recent works for future experiments to pin down the parity of the Θ^+.

Acknowledgments

---

[1] T. Nakano *et al.* [LEPS Collaboration], Phys. Rev. Lett. **91**, 012002 (2003)

[2] D. Diakonov, V. Petrov and M. V. Polyakov, Z. Phys. A **359**, 305 (1997)

[3] V. V. Barmin *et al.* [DIANA Collaboration], Phys. Atom. Nucl. **66**, 1715 (2003) [Yad. Fiz. **66**, 1763 (2003)]

[4] S. Stepanyan *et al.* [CLAS Collaboration], Phys. Rev. Lett. **91**, 252001 (2003);
V. Kubarovsky *et al.* [CLAS Collaboration], hep-ex/0307088

[5] J. Barth [SAPHIR Collaboration], hep-ex/0307083

[6] A. Airapetian *et al.* [HERMES Collaboration], hep-ex/0312044

[7] A. Aleev *et al.* [SVD Collaboration], hep-ex/0401024

[8] A. E. Asratyan, A. G. Dolgolenko and M. A. Kubantsev, hep-ex/0309042

[9] C. Alt *et al.* [NA49 Collaboration], hep-ex/0310014

[10] R.L. Jaffe and F. Wilczek, Phys. Rev. Lett. **91**, 232003 (2003) ;
M. Karliner and H. Lipkin, hep-ph/0307243;
S. Capstick, Ph.R. Page and W. Roberts, Phys. Lett. **B570**, 185 (2003);
C.E. Carlson, Ch.D. Caronne, H.J. Kwee and V. Nazaryan, Phys. Lett. **B573**, 101 (2003);
E. Shuryak and I. Zahed, hep-ph/0310270

[11] M. Praszałowicz, talk at *Workshop on Skyrmions and Anomalies*, M. Jeżabek and M. Praszałowicz eds., World Scientific 1987, page 112 and Phys. Lett. **B575**, 234 (2003);
H. Weigel, Eur. Phys. J. **A2**, 391 (1998);
H. Walliser and V.B. Kopeliovich, Nucl. Phys. **B660**, 156 (2003);
A. Hosaka, Phys. Lett. B **571**, 55 (2003);
D. Diakonov and V. Petrov, hep-ph/0309203;
H.- Ch. Kim and M. Praszłowicz, hep-ph/0308242, to appear in Phys. Lett. B

[12] N. Itzhaki, I.R. Klebanov, P. Ouyang and L. Rastelli, hep-ph/0309305

[13] D.E. Kahana and S.H. Kahana, hep-ph/0310026;
F. Huang, Z. Y. Zhang, Y. W. Yu and B. S. Zou, hep-ph/0310040

[14] S. L. Zhu, Phys. Rev. Lett. **91**, 232002 (2003) ;
J. Sugiyama, T. Doi and M. Oka, Phys. Lett. B **581**, 167 (2004)

[15] F. Csikor, Z. Fodor, S. D. Katz and T. G. Kovacs, JHEP **0311**, 070 (2003);
S. Sasaki, hep-lat/0310014

[16] Y. Oh, H. Kim and S. H. Lee, Phys. Rev. D**69** 014009, (2004) ;
T. Hyodo, A. Hosaka and E. Oset, Phys. Lett. B **579**, 290 (2004);
S. I. Nam, A. Hosaka and H.- Ch. Kim, Phys. Lett. B **579**, 43 (2004)

[17] W. Liu and C. M. Ko, Phys. Rev. C 68045203, (2003)

[18] K. Nakayama and K. Tsushima, hep-ph/0311112

[19] A. W. Thomas, K. Hicks and A. Hosaka, hep-ph/0312083, to appear in Prog. Theor. Phys.

[20] C. Hanhart *et al.*, hep-ph/0312236

[21] Q. Zhao and J. S. Al-Khalili, hep-ph/0312348

[22] B. G. Yu, T. K. Choi and C. R. Ji, nucl-th/0312075

[23] C. E. Carlson, C. D. Carone, H. J. Kwee and V. Nazaryan, hep-ph/0312325

[24] S. I. Nam, A. Hosaka and H. C. Kim, hep-ph/0401074

[25] T. Mehen and C. Schat, hep-ph/0401107

[26] M. P. Rekalo and E. Tomasi-Gustafsson, hep-ph/0401162

[27] Private communication with T. Nakano

[28] M. V. Polyakov, A. Sibirtsev, K. Tsushima, W. Cassing and K. Goeke, Eur. Phys. J. A **9**, 115 (2000)

[29] W. Liu and C. M. Ko, Phys. Rev. C **68**, 045203 (2003)

[30] Y. Oh, H. Kim and S. H. Lee, hep-ph/0311054

[31] M. Bleicher, F. M. Liu, J. Aichelin, T. Pierog and K. Werner, hep-ph/0401049

[32] W. Liu, C. M. Ko and V. Kubarovsky, nucl-th/0310087

[33] V. G. J. Stokes and Th. A. Rijken, Phys. Rev. C **59**, 3009 (1999)

[34] A. Reuber, K. Holinde and J. Speth, Nucl. Phys. A **570**, 543 (1994)

[35] R. Machleidt, K. Holinde and C. Elster, Phys. Rept. **149**, 1 (1987)

[36] W. Liu, C. M. Ko and S. H. Lee, Nucl. Phys. A **728**, 457 (2003)

[37] G. Penner and U. Mosel, Phys. Rev. C **66**, 055211 (2002)